Electronic Supplementary Material (ESI) for ChemComm.

Mesoporous Perovskite Titanates via Hydrothermal Conversion

Tianyu Li and Efrain E. Rodriguez*

Department of Chemistry and Biochemistry, University of Maryland,

College Park, Maryland 20742-2115, USA

Supplementary Information

1. Characterization method

Transmission electron microscopy (TEM) image was taken using JEOL JEM 2100 LaB6 TEM equipment. Powder XRD pattern was recorded on the Bruker D8 Advance diffractometer, with Cu Kα/Kb radiation. Rietveld refinement was performed using TOPAS 5[1]. The nitrogen adsorption isotherms were measured by Micromeritics ASAP 2020 Porosimeter Test Station. Surface area was calculated by applying Brunauer−Emmett−Teller (BET) equation on adsorption data obtained at P/P_0 between 0.05 and 0.35. The pore size distributions were calculated by analyzing the adsorption branch of the N_2 sorption isotherm using the Barret−Joyner−Halenda (BJH) method. X-ray Small angle scattering (SAXS) pattern was collected by Xenocs Xeuss SAXS/WAXS/GISAXS small angle system. TEM image, electron diffraction, XRD and pore size distribution of $SrTiO_3$ materials synthesized from different method are summarized in **Figure S1.**

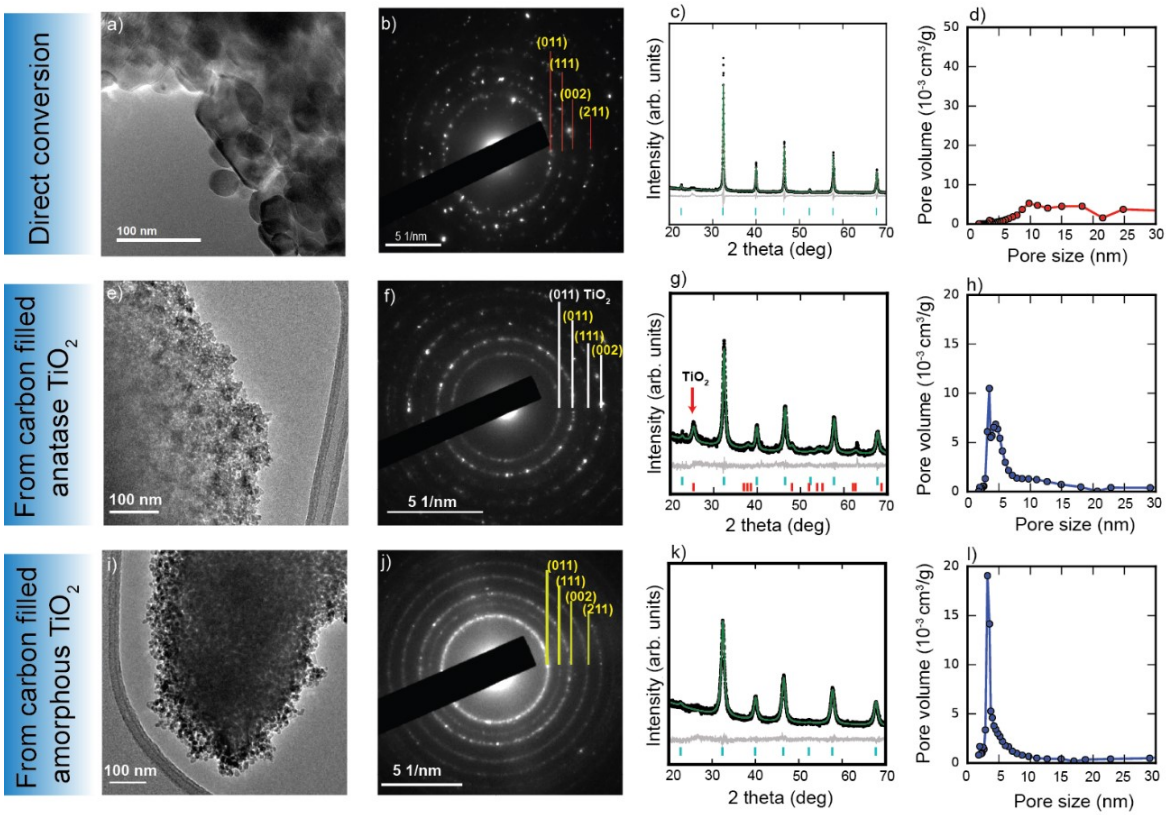

Figure S1. TEM image, electron diffraction, XRD and pore size distribution of $SrTiO_3$ materials synthesized from a)-d) Direct hydrothermal conversion of mesoporous crystalline TiO_2. e)-h) Hydrothermal conversion of mesoporous crystalline TiO_2 after filling carbon support into pores. i)-l) Hydrothermal conversion of mesoporous amorphous TiO_2 after filling carbon support into pores.

2. Synthesis of mesoporous crystalline TiO_2

Mesoporous crystalline TiO_2 was synthesized via a reported evaporation-induced self-assembly (EISA) method[2] . Typically, 0.8 g of triblock copolymer Pluronic P127 was first added into 12 mL of anhydrous ethanol (EtOH), followed by the addition of 1.2g acetic acid and 1.2 g concentrated hydrochloric acid (HCl, 37%). After stirring for 0.5 h at room temperature, 5 mmol (≈ 1.4 ml) Titanium butoxide $Ti(C_4H_9O)_4$ was slowly added to the solution dropwise. The above solution was under with vigorous stirring for around 3 h. The resulting sol solution was transferred in an open glass container (diameter 2 inch) and was later placed in 40 ºC environment and 60 ºC environment each for 24 h, allowing the evaporation of the solvent to form gel. The Mesoporous TiO_2 powder was obtained by calcinating the formed gel at 350 ºC for 4h (1ºC/min ramping) with enough air provided. The basic characterization of mesoporous crystalline TiO_2 is displayed in **Figure S2**.

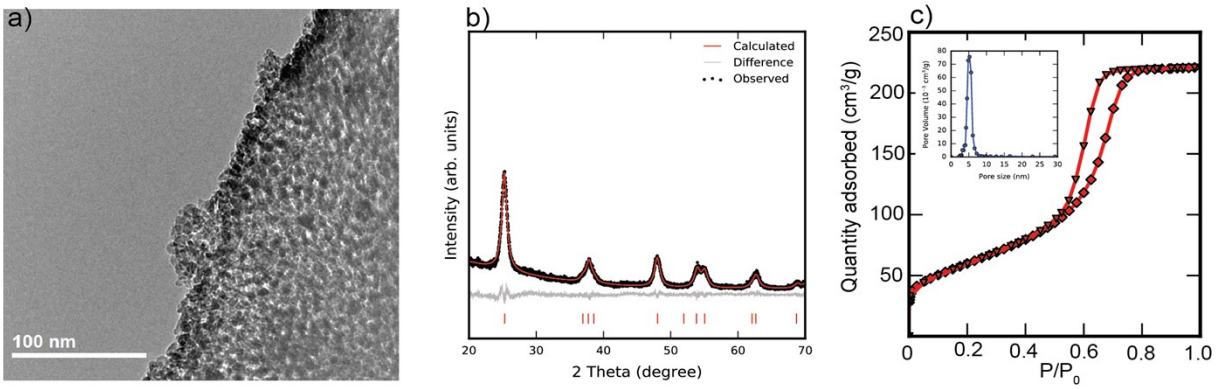

Figure S2. TEM (a), XRD with Rieltveld refinement (b) and Nitrogen adsorption isotherm (pore size distribution in inset) (c) for mesoporous crystalline TiO_2.

3. Direct hydrothermal conversion of mesoporous crystalline TiO_2 into $SrTiO_3$.

0.2g mesoporous crystalline TiO_2 and 0.8g $Sr(OH)_2$ are mixed in the 15ml water and the mixture undergoes hydrothermal treatment at 200 °C for 24h. The obtained solid is washed first with 5% acetic acid solution for 3 times to remove unreacted $Sr(OH)_2$ and $SrCO_3$ then with water for another 3 times. The $SrTiO_3$ product is dried in air at 80°C. Characterizations are shown in **Figure 1a-d and Figure S1a-d.** Nitrogen adsorption isotherm and pore size

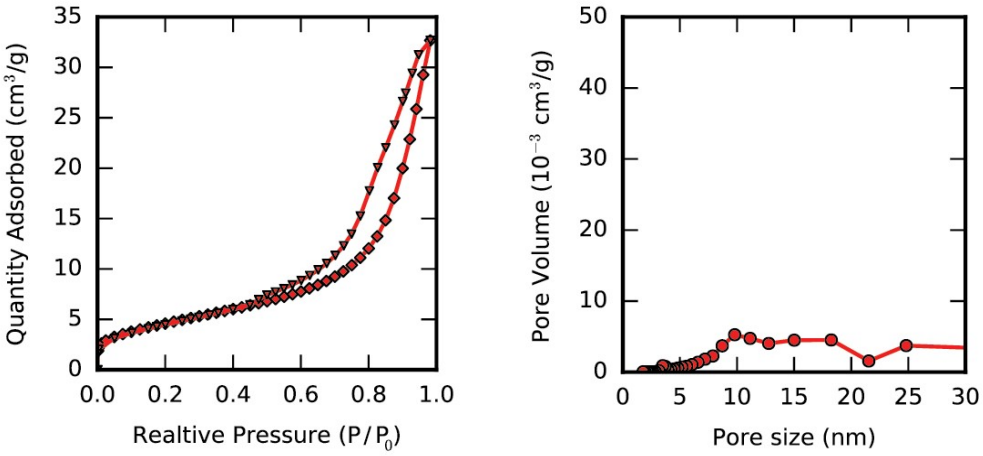

Figure S3. (a)Nitrogen adsorption isotherm and pore size distribution for (b) $SrTiO_3$ from direct hydrothermal conversion of mesoporous crystalline TiO_2.

distribution are displayed in **Figure S3.**

4. Hydrothermal conversion of carbon filled mesoporous crystalline TiO_2 into $SrTiO_3$.

4.1 Filling mesoporous crystalline TiO_2 with carbon.

Carbon filling is achieved via an impregnation method. 0.2g mesoporous crystalline TiO_2 is added to a solution obtained by dissolving 0.2g of sucrose and 1 drop of H_2SO_4 (~0.05 ml) 2

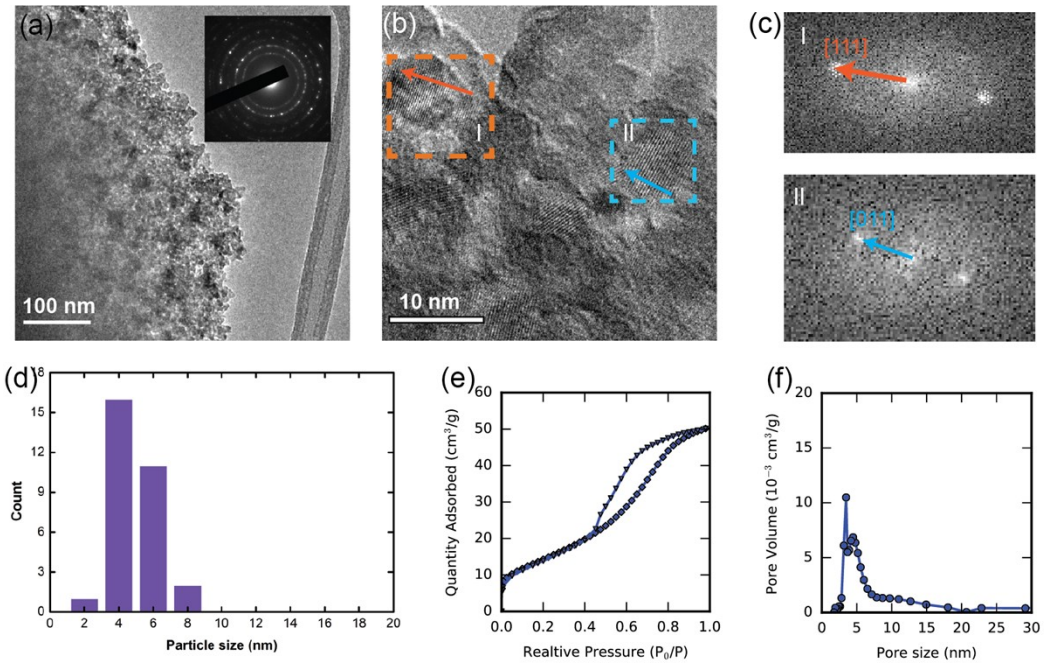

Figure S4. (a)TEM, (b) High resolution TEM, (c) Fourier Transform of the High-resolution TEM, (d) grain size distribution, (e) Nitrogen adsorption isotherm and pore size distribution for $SrTiO_3$ from hydrothermal conversion of carbon filled mesoporous crystalline TiO_2.

ml H_2O. After 5 min sonication, the mixture is placed in an oven for 6 h at 100°C. Subsequently, the temperature is increased to 180°C and maintained for another 6 h.

4.2 Conversion of carbon filled mesoporous crystalline TiO_2 into $SrTiO_3$.

0.2g carbon filled mesoporous crystalline TiO_2 and 0.8g $Sr(OH)_2$ are mixed in the 15ml water and the mixture undergoes hydrothermal treatment at 200 °C for 24h. The obtained solid is washed first with 5% acetic acid solution for 3 times to remove unreacted $Sr(OH)_2$ and $SrCO_3$ then with water for another 3 times. The product is dried in air at 80°C. The final $SrTiO_3$ product is obtained after 4h calcination at 450 °C in air to remove the carbon. characterizations are

shown in **Figure 1e-h, S2e-h and S4.** XRD pattern is displayed in **Figure S5a.** Due to the existence of TiO_2 impurity observed in the sample, we tried to increase the hydrothermal treatment time to 96h. The XRD pattern of resulting samples is shown in **Figure S5b.**

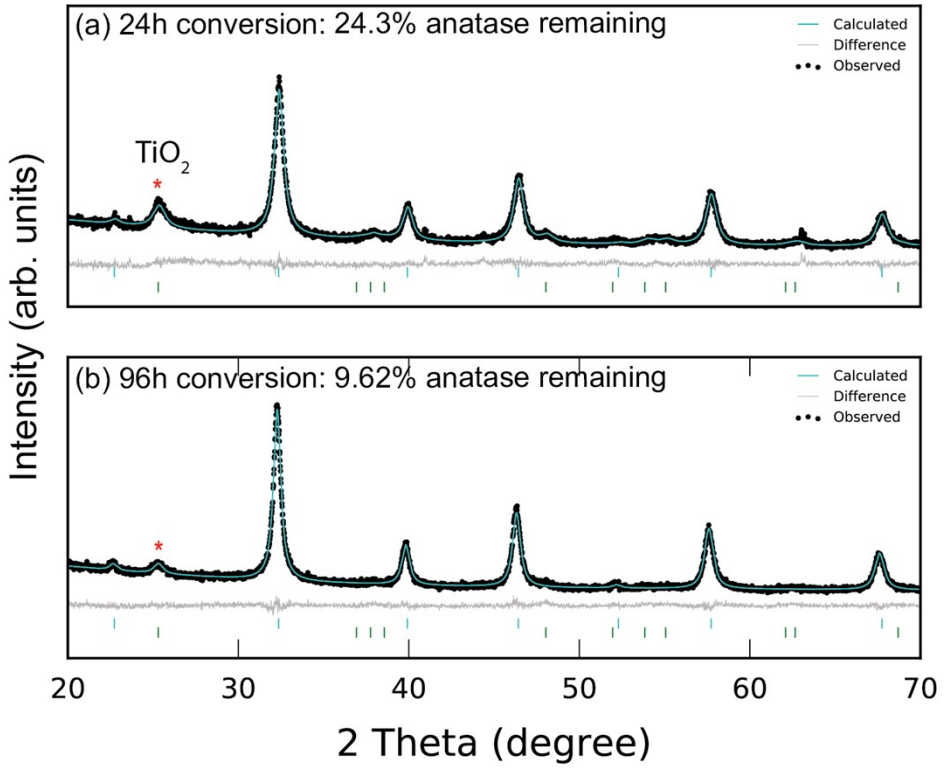

Figure S5. XRD with Rieltveld refinement for (a) $SrTiO_3$ from hydrothermal conversion of carbon filled mesoporous crystalline TiO_2 for 24h. (b) $SrTiO_3$ from hydrothermal conversion of carbon filled mesoporous crystalline TiO_2 for 96h.

5. Synthesis of mesoporous amorphous TiO_2

Mesoporous amorphous TiO_2 was synthesized via a reported evaporation-induced self-assembly (EISA) method[3]. Typically, 0.8 g of triblock copolymer Pluronic P127 was first added into 12 mL of anhydrous ethanol (EtOH), followed by the addition of 1.2g acetic acid and 1.2 g concentrated hydrochloric acid (HCl 37%). After stirring for 0.5 h at room temperature, 5 mmol (≈ 1.4 ml) Titanium butoxide $Ti(C_4H_9O)_4$ was slowly added to the solution dropwise. The above solution was under with vigorous stirring for around 3 h. The resulting sol solution was transferred in an open glass container (diameter 2 inch) and was later placed in a 40 °C environment and a 60 °C environment each for 24 h, allowing the evaporation of the solvent to form gel. The Mesoporous TiO_2 powder was obtained by calcinating the formed

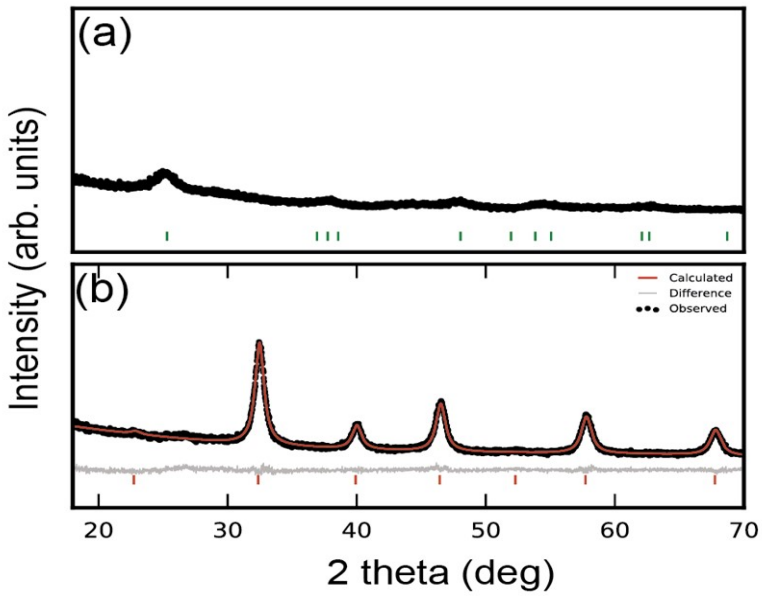

Figure S6. XRD with Rieltveld refinement for (a) mesoporous amorphous TiO_2 (b) $SrTiO_3$ from hydrothermal conversion of carbon filled mesoporous amorphous TiO_2 for 24h. No impurity of TiO_2 is observed.

gel at 350 ºC for 4h (1°C/min ramping) in the N_2 flow environment. XRD pattern of the sample is presented in **Figure S6a**. Nitrogen adsorption isotherm and pore size distribution are displayed in **Figure S7** (blue curve).

6. Hydrothermal conversion of carbon filled mesoporous amorphous TiO_2 into $SrTiO_3$

6.1 Filling mesoporous amorphous TiO_2 with carbon.

0.2g mesoporous amorphous TiO_2 is added to a solution obtained by dissolving 0.2g of sucrose and 1 drop of H_2SO_4 (~0.05 ml) 2 ml H_2O. After 5 min sonication, the mixture is placed in an oven for 6 h at 100°C. Subsequently, the temperature is increased to 180°C and maintained for another 6 h.

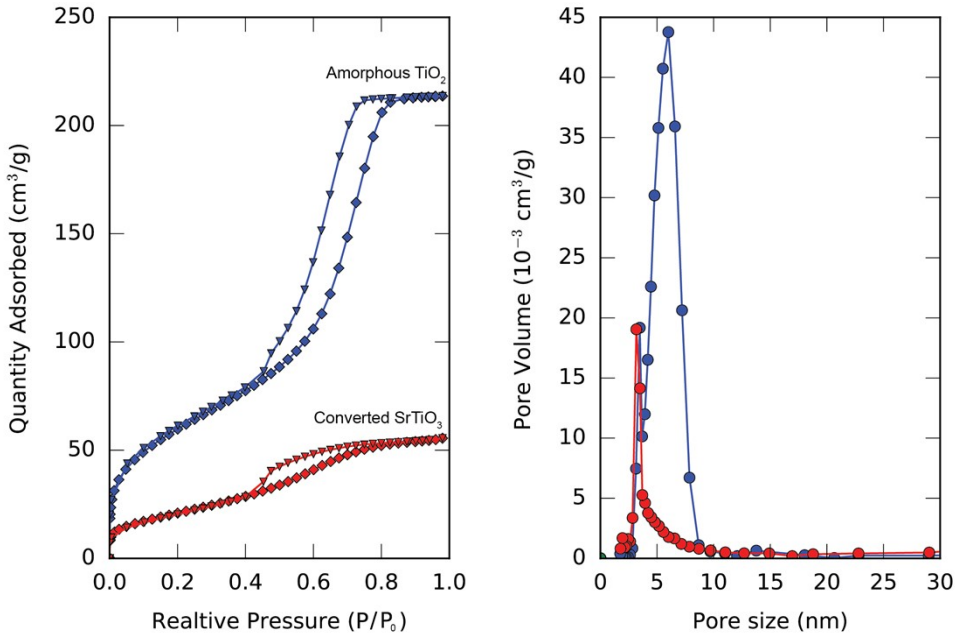

Figure S7. Nitrogen adsorption isotherm (left) and pore size distribution(right) of mesoporous amorphous TiO_2 (blue curve) $SrTiO_3$ from hydrothermal conversion of carbon filled mesoporous amorphous TiO_2 for 24h (red curve).

6.2 Conversion of carbon filled mesoporous amorphous TiO_2 into $SrTiO_3$.

0.2g carbon filled mesoporous amorphous TiO_2 and 0.8g $Sr(OH)_2$ are mixed in the 15ml water and the mixture undergoes hydrothermal treatment at 200 °C for 24h. The obtained solid is washed first with 5% acetic acid solution for 3 times to remove unreacted $Sr(OH)_2$ and $SrCO_3$ then with water for another 3 times. The product is dried in air at 80°C. The final $SrTiO_3$ product is obtained after 4h calcination at 450 °C in air to remove the carbon. Characterizations are shown in **Figure 1i-l**, **Figure S2i-l and Figure S8.** XRD pattern is displayed in **Figure S6a.** Nitrogen adsorption isotherm and pore size distribution are displayed in **Figure S7** (red curve). To verify there is no amorphous TiO_2 phase in the product, we calcinated both mesoporous amorphous TiO_2 and our mesoporous $SrTiO_3$ product in air at certain temperatures. Mesoporous amorphous TiO_2 is calcinated in air at 450 °C for 4h and XRD (**Figure S9b)** shows it crystalized into anatase phase after calcination. However, for the mesoporous $SrTiO_3$ product, no other crystalline phase appears even after 8h calcination at 650°C in air **(Figure S10**), confirming TiO_2 is fully converted to $SrTiO_3$ after hydrothermal treatment.

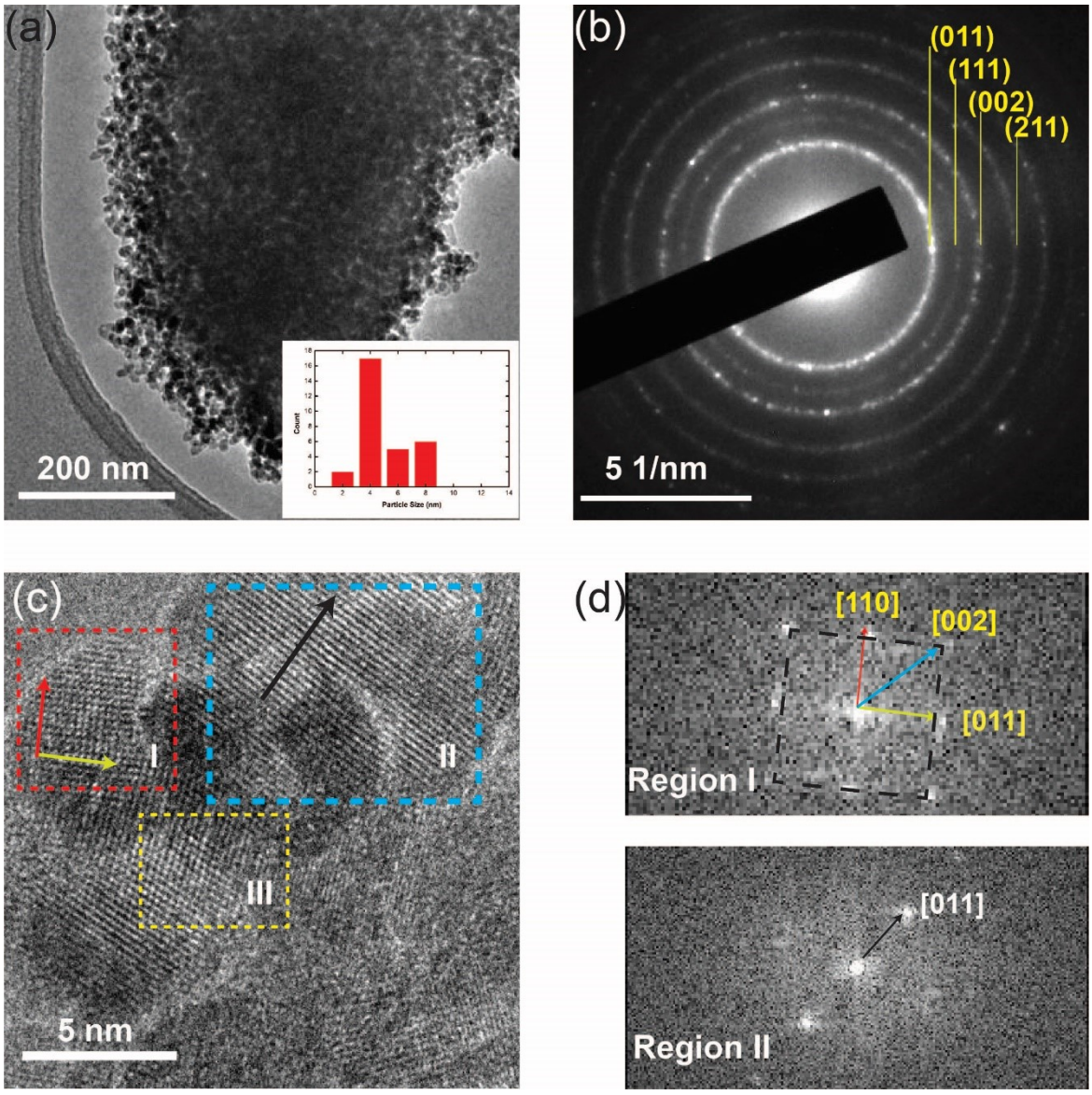

Figure S8. (a) TEM with particle distribution (b) Electron diffraction (c) High resolution TEM, (d) Fourier Transform of the High-resolution TEM $SrTiO_3$ from hydrothermal conversion of carbon filled mesoporous TiO_2.

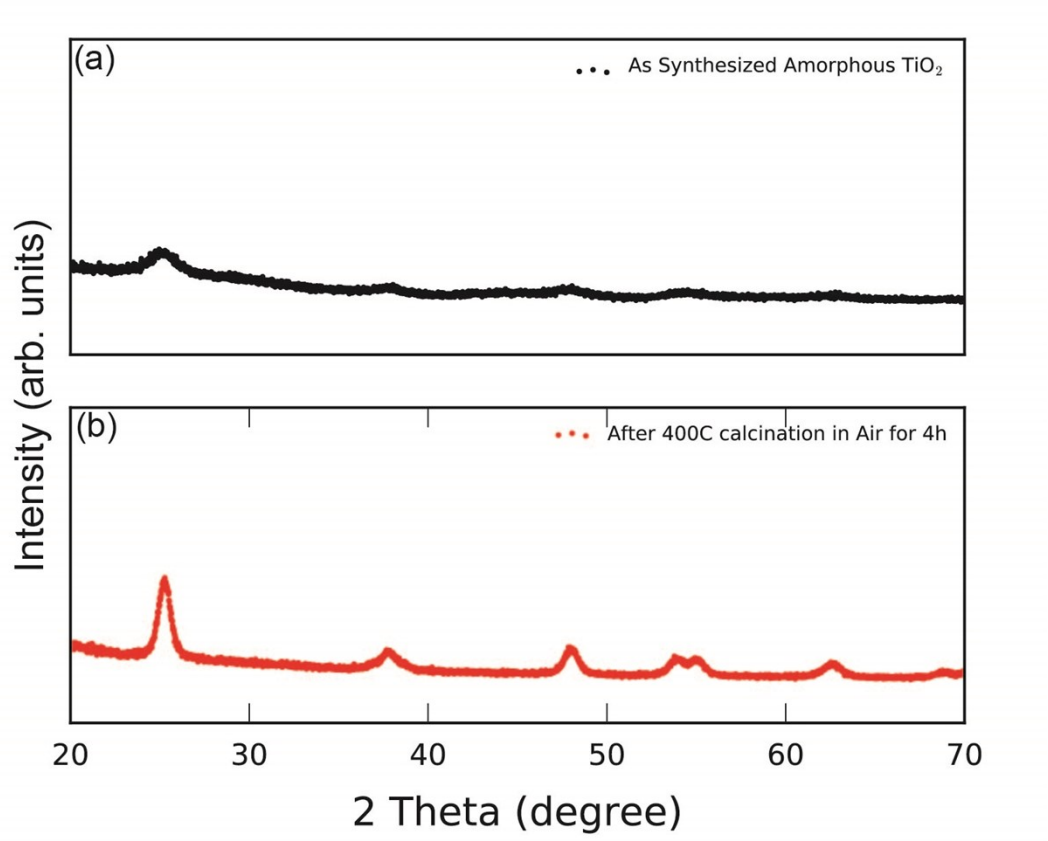

Figure S9. XRD for (a) mesoporous amorphous TiO_2 and (b) the product obtained by calcinating mesoporous amorphous TiO_2.at 450 °C for 4h in air.

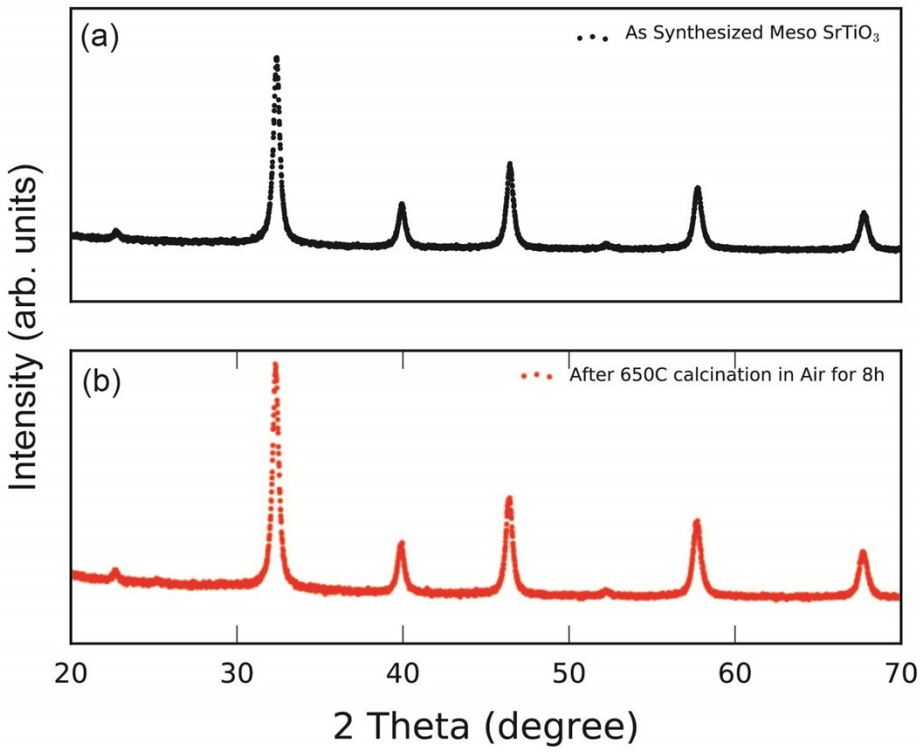

Figure S10. XRD for $SrTiO_3$ from hydrothermal conversion of carbon filled mesoporous amorphous TiO_2 for 24h (a) before and (b) after calcination at 650°C in air for 8h.

Sample Information	Refined crystal size (nm)	Surface area (m^2/g)	Pore volume (cm^3/g)
Crystalline mesoporous TiO_2	10.5(2)	205.7	0.345
$SrTiO_3$ from direct conversion crystalline mesoporous TiO_2	49.1(1)	15	0.0498
$SrTiO_3$ from conversion crystalline mesoporous TiO_2 after filling carbon	16.6(6)	53.2	0.0774
Amorphous mesoporous TiO_2	/	213.4	0.309
$SrTiO_3$ from conversion Amorphous mesoporous TiO_2 after filling carbon	11.6	77.4	0.082

Table S1. Refined crystal size, surface area and mean pore size of synthesized mesoporous TiO_2 and $SrTiO_3$ samples.

7. Synthesis of carbon/amorphous TiO_2 composite and their conversion into $SrTiO_3$.

7.1 Synthesis of carbon/amorphous TiO_2 composite

0.8 g of triblock copolymer Pluronic P127 was first added into 12 mL of anhydrous ethanol (EtOH), followed by the addition of 1.2g acetic acid and 1.2 g concentrated hydrochloric acid (HCl 37%). After stirring for 0.5 h at room temperature, 5 mmol (≈ 1.4 ml) Titanium butoxide $Ti(C_4H_9O)_4$ was slowly added to the solution dropwise. Followed is the addition of certain mass ratio of sucrose into the solution. The above solution was under with vigorous stirring for around 3 h. The resulting sol solution was transferred in an open glass container (diameter 2 inch) and was later placed in a 40 ºC environment and a 60 ºC environment each for 24 h, allowing the evaporation of the solvent to form gel. The Mesoporous TiO_2 powder was obtained by calcinating the formed gel at 350 ºC for 4h (1ºC/min ramping) in the N_2 flow environment. Basic characterizations are presented in **Figure S11.**

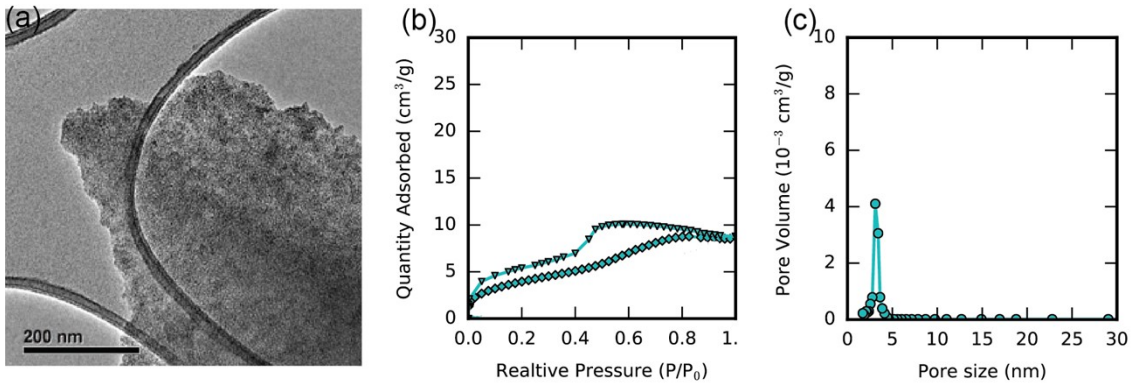

Figure S11. (a)TEM, (b) Nitrogen adsorption isotherm and (c) pore size distribution for carbon/amorphous TiO_2 composite.

7.2 Filling carbon/amorphous TiO_2 composite with carbon.

0.2g carbon/amorphous TiO_2 composite is added to a solution obtained by dissolving 0.2g of sucrose and 1 drop of H_2SO_4 (~0.05 ml) 2 ml H_2O. After 5 min sonication, the mixture is placed in an oven for 6 h at 100°C. Subsequently, the temperature is increased to 180°C and maintained for another 6 h.

7.3 Conversion of carbon/amorphous TiO_2 composite to $SrTiO_3$.

0.2g carbon/amorphous TiO_2 composite (carbon filled or not) and 0.8g $Sr(OH)_2$ are mixed in the 15ml water and the mixture undergoes hydrothermal treatment at 200 °C for 24h. The obtained solid is washed first with 5% acetic acid solution for 3 times to remove unreacted $Sr(OH)_2$ and $BaCO_3$ then with water for another 3 times. The product is dried in air at 80°C. The final $BaTiO_3$ product is obtained after 4h calcination at 450 °C in air to remove the carbon. Figure **S12** shows comparison of Nitrogen adsorption and pore size distribution data of $SrTiO_3$ converted from carbon/amorphous TiO_2 composite and carbon filled carbon/amorphous TiO_2 composite. TEM image of $SrTiO_3$ converted from carbon/amorphous TiO_2 composite is displayed in Figure **S13**. TEM image of $SrTiO_3$ converted from carbon filled carbon/amorphous TiO_2 composite is displayed in Figure **S14**. Comparison of Nitrogen adsorption and pore size distribution data of $SrTiO_3$ converted from d carbon filled carbon/amorphous TiO_2 composite and carbon filled mesoporous amorphous TiO_2 is presented in Figure **S15**. Carbon/amorphous TiO_2 composite in the characterization here is synthesized via 1:10 sucrose/titanium butoxide ratio.

Sample Information	Refined crystal size (nm)	Surface area (m^2/g)	Pore volume (cm^3/g)
TiO_2/C composite from 1:10 sucrose/titanium butoxide ratio	/	14.14	0.0115
$SrTiO_3$ from direct conversion of TiO_2/C composite	23.7	54.3	0.2018
$SrTiO_3$ from conversion of TiO_2/C composite after filling carbon	16.6	73.4	0.1708

Table S2. Refined crystal size, surface area and mean pore size of synthesized TiO_2/C composite and its converted $SrTiO_3$ samples.

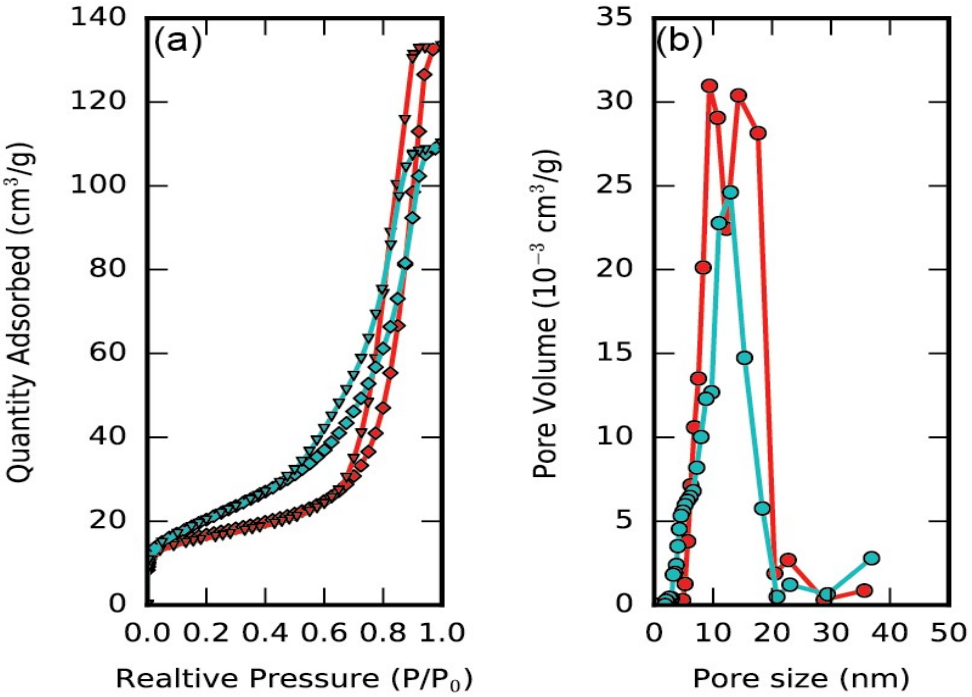

Figure S12. Nitrogen adsorption isotherm (left) and pore size distribution(right) of mesoporous $SrTiO_3$ from direct hydrothermal conversion of TiO_2/C composite (red curve). crystalline TiO_2. Mesoporous $SrTiO_3$ from hydrothermal conversion of TiO_2/C composite after filling carbon (blue curve).

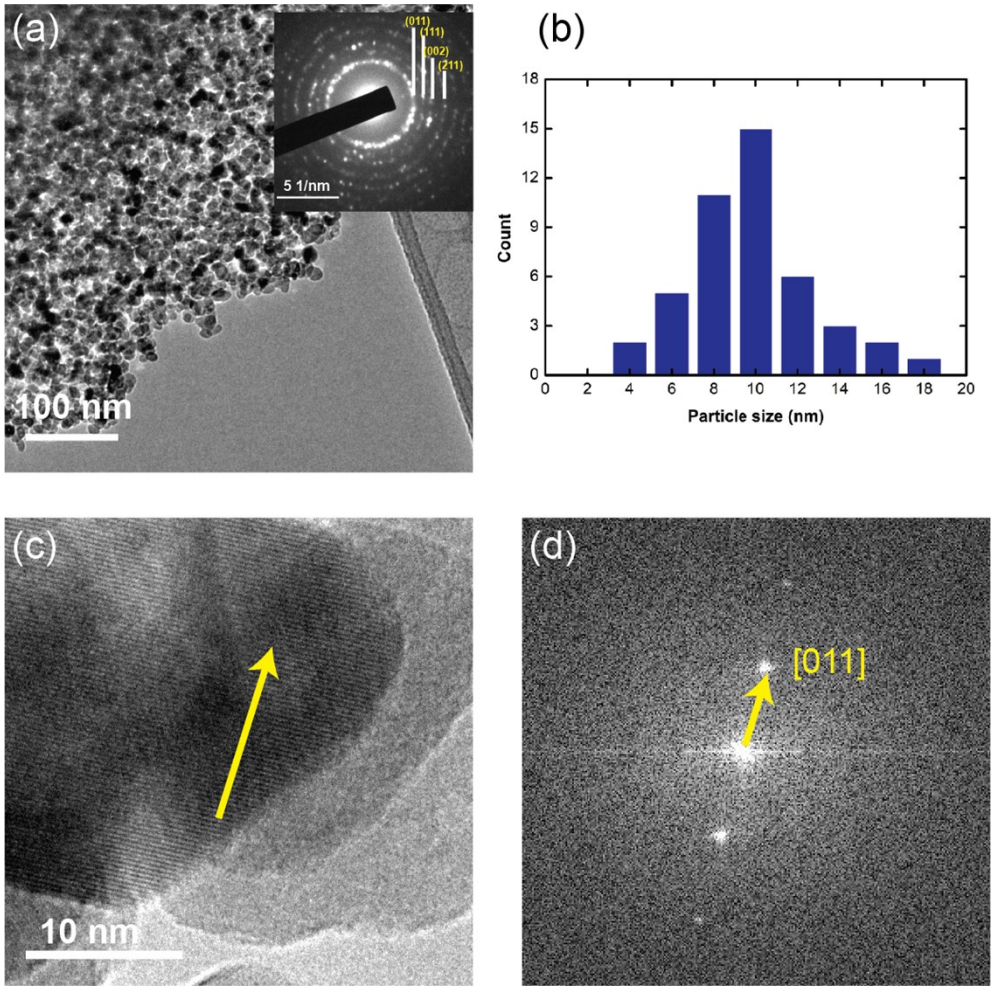

Figure S13. (a) TEM, (b) grain size distribution, (c) High resolution TEM, (d) Fourier Transform of the High-resolution TEM $SrTiO_3$ from hydrothermal conversion of TiO_2/C composite.

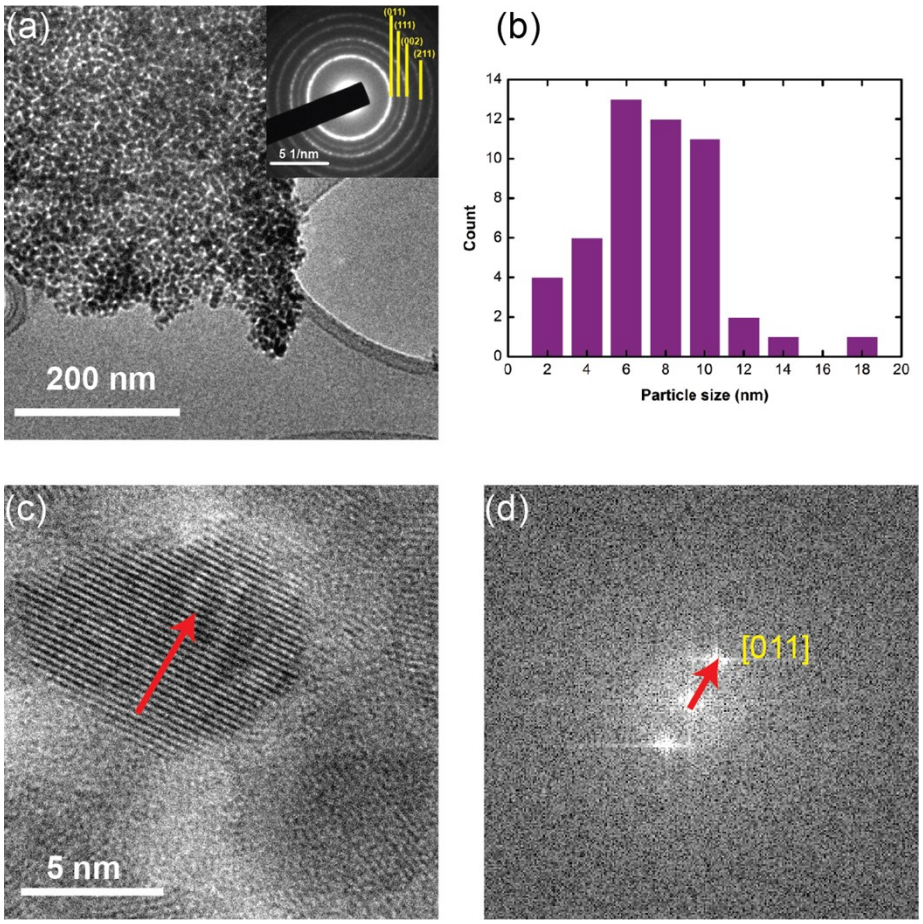

Figure S14. (a) TEM, (b) grain size distribution, (c) High resolution TEM, (d) Fourier Transform of the High-resolution TEM $SrTiO_3$ from hydrothermal conversion of TiO_2/C composite after carbon filling.

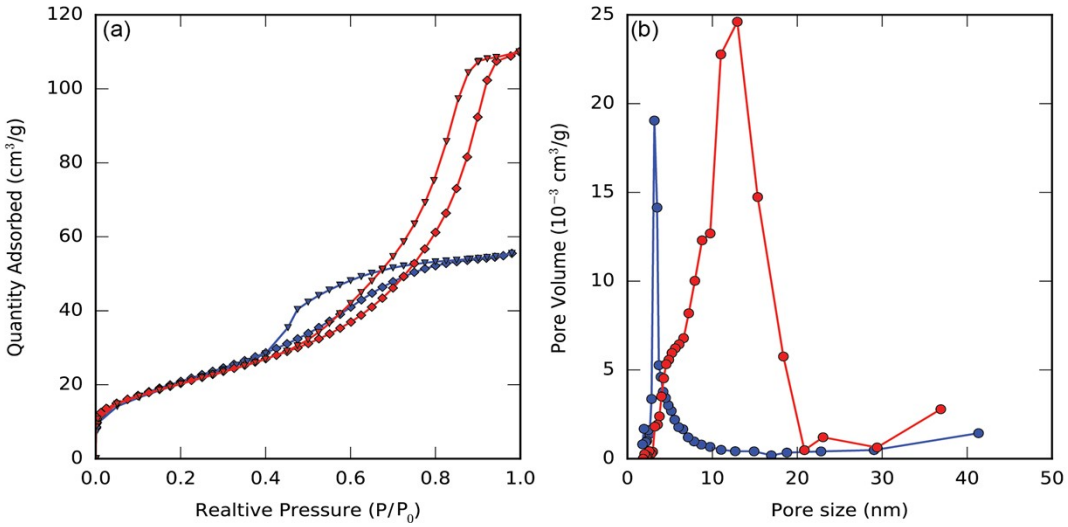

Figure S15. Nitrogen adsorption isotherm (left) and pore size distribution(right) of mesoporous $SrTiO_3$ from hydrothermal conversion of Mesoporous $SrTiO_3$ from hydrothermal conversion of TiO_2/C composite after filling carbon (red curve). Mesoporous $SrTiO_3$ from hydrothermal conversion of carbon filled mesoporous amorphous TiO_2 for 24h (blue curve).

Mass Ratio (titanium butoxide vs. sucrose)	Mean pore size(nm)	Surface area (m^2/g)	Surface area (m^2/mol)	Pore volume (cm^3/g)	Pore volume (cm^3/mol)
1:10	3.9	73.4	13465.964	0.17	31.1882
0.75:10	4.1	127.8	23446.188	0.18	33.0228
0.5:10	5.2	111.2	20400.752	0.15	27.519
0.25:10	7.6	81.5	14951.99	0.15	27.519
0.125:10	9.7	109.7	20125.562	0.11	20.1806
0:10	12.8	77.4	14199.804	0.082	15.04372
Comparison Amorphous mesoporous TiO_2	6.1	213.4	16008.38	0.309	56.68914

Table S3. Comparison of mean pore size, surface area and pore volume of $SrTiO_3$ from hydrothermal conversion of carbon filled TiO_2/C composite when different sucrose/titanium butoxide ratio is used for the synthesis of TiO_2/C composite.

8. Hydrothermal conversion of carbon filled mesoporous amorphous TiO_2 into $BaTiO_3$.

0.2g carbon filled amorphous C/TiO_2 and 1g $Ba(OH)_2$ are mixed in the 15ml water and the mixture undergoes hydrothermal treatment at 200 °C for 24h. The obtained solid is washed first with 5% acetic acid solution for 3 times to remove unreacted $Ba(OH)_2$ and $BaCO_3$ then with water for another 3 times. The product is dried in air at 80°C. The final $BaTiO_3$ product is obtained after 4h calcination at 450 °C in air to remove the carbon. Characterizations of $BaTiO_3$ using 0.5:10 sucrose/titanium butoxide ratio are shown in **Figure S16.** Comparison of Nitrogen adsorption and pore size distribution data of $BaTiO_3$ synthesized using different

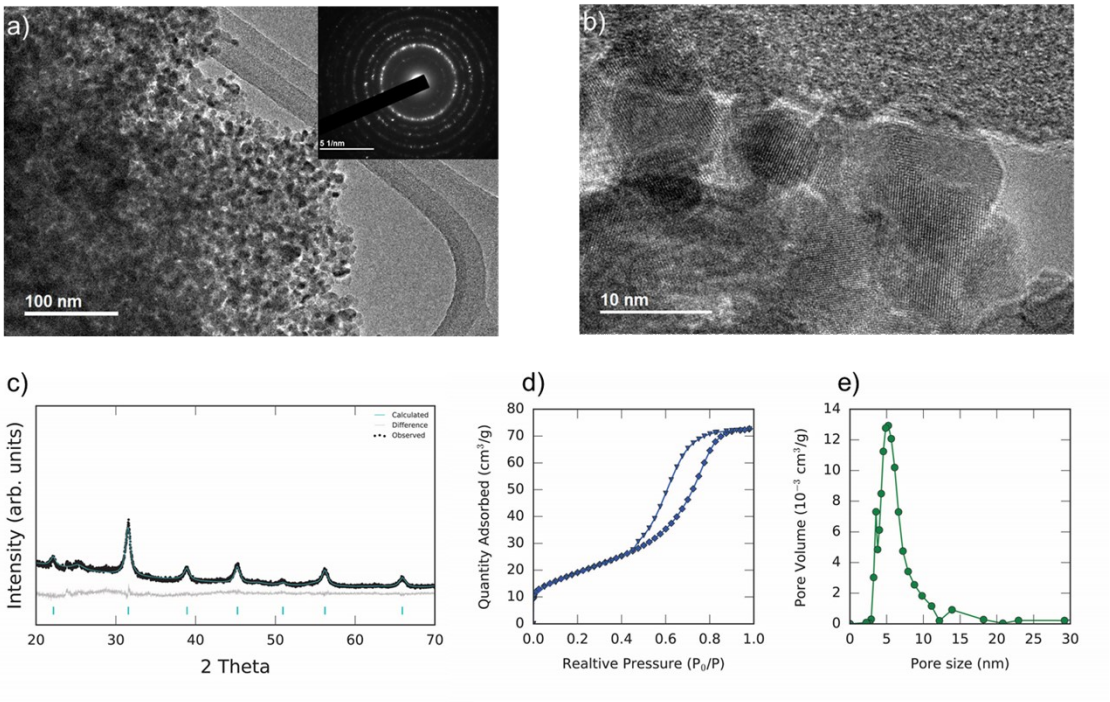

Figure S16. (a)TEM, (b) High resolution TEM, (c) XRD with Rietveld refinement, (d)Nitrogen adsorption isotherm and (e) pore size distribution for $BaTiO_3$ from hydrothermal conversion of TiO_2/C composite after filling carbon.

sucrose/titanium butoxide ratio is shown in Figure **S17**.

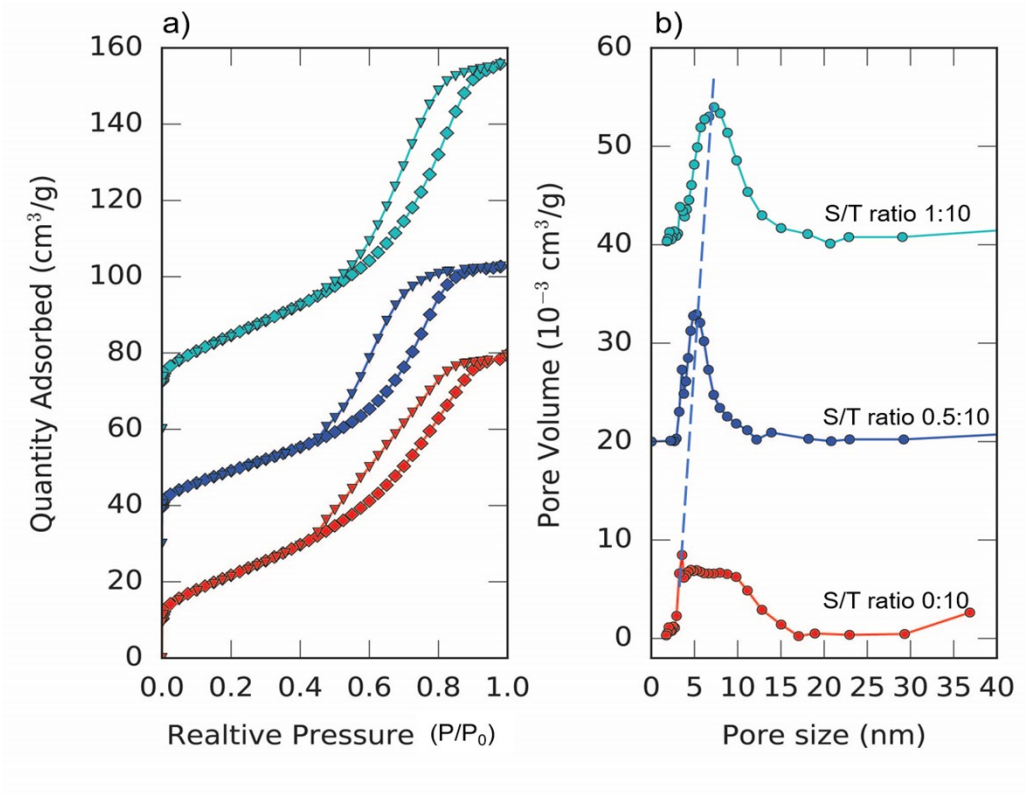

Figure S17. Nitrogen adsorption isotherm (left) and pore size distribution(right) of mesoporous $BaTiO_3$ from hydrothermal conversion carbon filled TiO_2/C composite when different sucrose/titanium butoxide ratio is used for the synthesis of TiO_2/C composite.

Mass Ratio (titanium butoxide vs. sucrose)	Mean pore szie (nm)	Surface area (m^2/g)	Surface area (m^2/mol)	Pore volume (cm^3/g)	Pore volume (cm^3/mol)
0:10	3.2	68.8	16093.696	0.113	26.350696
0.5:10	5.4	80.27	18776.7584	0.122	28.449424
1:10	7.6	88.78	20767.4176	0.149	34.745608
Comparison amorphous mesoporous TiO_2	6.1	213.4	16008.38	0.309	56.68914

Table S4. Comparison of mean pore size, surface area and pore volume of $BaTiO_3$ from hydrothermal conversion of carbon filled TiO_2/C composite when different sucrose/titanium butoxide ratio is used for the synthesis of TiO_2/C composite.

9. Hydrothermal conversion of carbon filled mesoporous amorphous TiO_2 into Li_2TiO_3.

0.2g carbon filled amorphous C/TiO_2 (from 0.5:10 sucrose/titanium butoxide ratio) and 1g LiOH are mixed in the 15ml water and the mixture undergoes hydrothermal treatment at 200 °C for 24h. The obtained solid is washed first with 5% acetic acid solution for 3 times to remove unreacted LiOH and $BaCO_3$ then with water for another 3 times. The product is dried in air at 80°C. The final Li_2TiO_3 product is obtained after 4h calcination at 450 °C in air to remove the carbon. Characterizations are shown in **Figure S18.** The XRD indicates the Li_2TiO_3 is a

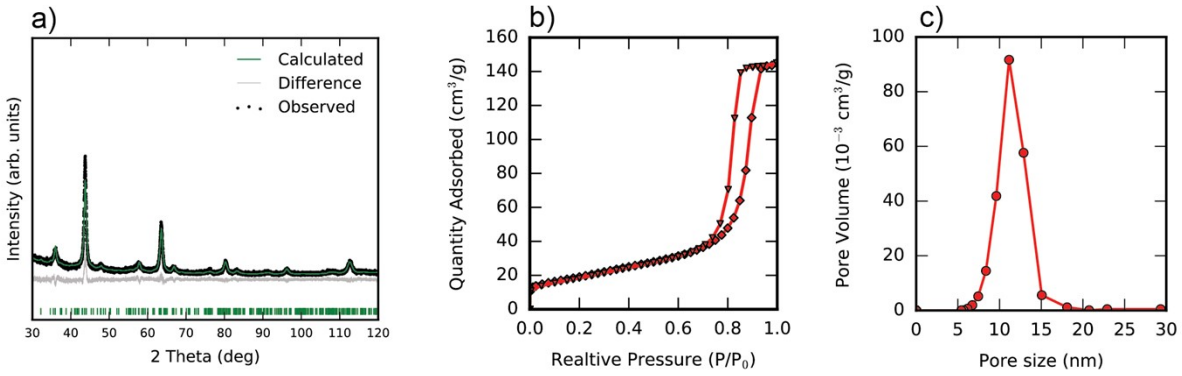

Figure S18. (a) XRD with its refinement (b) Nitrogen adsorption isotherm and (c) pore size distribution for Li_2TiO_3 from hydrothermal conversion of TiO_2/C composite after filling carbon.

monoclinic phase.

System	S_{bet} (m^2/g)	Reference
Mesoporous#	127	This work
Mesoporous	30-50*	4
Mesoporous	89.2	5
Nano particle#	11.2	6
Nano particle	42	7
Nano particle	20.8	8
Aerogel	175	9
Aerogel	370	10
Nano particle	27.4	11
Mesoporous	83	12
Mesoporous	108	13
Nano particle	18.5	14
Nano particle	21	15
Nano particle	37.4	16
Mesoporous	120	17
Nano particle	14	18
Nano particle	20	19

Table S5. Comparison of Surface areas of reported representative high surface area $SrTiO_3$ materials. #Mesoporous and nanoparticles are usually used together in the literature. * The study did not report BET surface area. However, they did nitrogen adsorption measurement. So we estimated the BET surface from their nitrogen adsorption isotherm curves.

References:

1 R. W. Cheary and A. Coelho, *J. Appl. Crystallogr.*, 1992, **2**, 109–121.

2 R. Liu, Y. Ren, Y. Shi, F. Zhang, L. Zhang, B. Tu and D. Zhao, *Chem. Mater.*, 2008, **20**, 1140–1145.

3 J. Liu, S. Pancera, V. Boyko, A. Shukla, T. Narayanan and K. Huber, *Langmuir*, 2010, **26**,

17405–17412.

4 B. Huang, Y. Liu, Q. Pang, X. Zhang, H. Wang and P. K. Shen, *J. Mater. Chem. A*, 2020, **8**, 22251–22256.

5 X. Wei, G. Xu, Z. Ren, Y. Wang, G. Shen and G. Han, *J. Am. Ceram. Soc.*, 2008, **91**, 299–302.

6 † Yawen Wang, † Hua Xu, † Xiaobing Wang, † Xi Zhang, † Huimin Jia, *,† and Lizhi Zhang and J. Qiu‡, *J. Phys. Chem. B*, 2006, **110**, 13835–13840.

7 U. Sulaeman, S. Yin and T. Sato, *Appl. Catal. B Environ.*, 2011, **105**, 206–210.

8 Q. Kuang and S. Yang, *ACS Appl. Mater. Interfaces*, 2013, **5**, 3683–3690.

9 D. Demydov and K. J. Klabunde, *J. Non. Cryst. Solids*, 2004, **350**, 165–172.

10 F. Rechberger, G. Ilari, C. Willa, E. Tervoort and M. Niederberger, *Mater. Chem. Front.*, 2017, **1**, 1662–1667.

11 K. Klauke, B. Kayaalp, M. Biesuz, A. Iannaci, V. M. Sglavo, M. D'Arienzo, S. Lee, J. Seo, W. Jung and S. Mascotto, *ChemNanoMat*, 2019, **5**, 948–956.

12 L. F. Da Silva, L. J. Q. Maia, M. I. B. Bernardi, J. A. Andrés and V. R. Mastelaro, *Mater. Chem. Phys.*, 2011, **125**, 168–173.

13 X. Wei, G. Xu, Z. Ren, C. Xu, W. Weng, G. Shen and G. Han, *J. Am. Ceram. Soc.*, 2010, **93**, 1297–1305.

14 J. Wang, S. Yin, Q. Zhang, F. Saito and T. Sato, *Solid State Ionics*, 2004, **172**, 191–195.

15 Q. Kuang and S. Yang, *ACS Appl. Mater. Interfaces*, 2013, **5**, 3683–3690.

16 W. Zhao, H. Wang, N. Liu, J. Rong, Q. Zhang, M. Li and X. Yang, *J. Am. Ceram. Soc.*, 2019, **102**, 981–987.

17 H. Zhan, Z.-G. Chen, J. Zhuang, X. Yang, Q. Wu, X. Jiang, C. Liang, M. Wu and J. Zou, *J. Phys. Chem. C*, 2015, **119**, 3530–3537.

18 G. S. Foo, Z. D. Hood and Z. Wu, *ACS Catal.*, 2017, **8**, 555–565.

19 J. A. Enterkin, W. Setthapun, J. W. Elam, S. T. Christensen, F. A. Rabuffetti, L. D. Marks, P. C. Stair, K. R. Poeppelmeier and C. L. Marshall, *ACS Catal.*, 2011, **1**, 629–635.